LA-3432-MS
UC-48, BIOLOGY
AND MEDICINE
TID-4500 (46th Ed.)

LOS ALAMOS SCIENTIFIC LABORATORY
of the
University of California
LOS ALAMOS • NEW MEXICO

Report written: July 1965
Report distributed: December 20, 1965

Biological and Medical Research Group (H-4) of the Health Division -- Annual Report July 1964 Through June 1965

Group Leader, W. H. Langham
Division Leader, T. L. Shipman

CHAPTER 1

INTRODUCTION

(a) Program Orientation

The biological and medical research program is divided roughly into two general categories: fundamental and programmatic or applied investigations. The former, which now represents about 65 percent of the group's effort, is directed toward studies of biological phenomena at the molecular- and cellular-levels; the latter is concerned largely with somatic and genetic effects of radiation, from both internal and external sources, on animals. These activities, although further subdivided on the basis of the general disciplines concerned, often involve considerable collaboration where the nature of the problem requires a multidisciplinary approach.

The increased emphasis during the past few years on molecular- and cellular-level studies instigated many new projects which are now producing interesting results. Expansion of this program has essentially leveled off, although a few key staff and technical positions remain to be filled. Additional laboratory and office space in the Health Research Laboratory will be realized during the coming year through transfer of the Industrial Hygiene and Field Studies Groups to their new facilities.

Somatic Effects of Radiation.--The Effective Residual Dose (ERD) concept of radiation injury is being studied through tests of mathematical models describing various biological reparable and irreparable injury conditions. Potential external and internal hazards from radioactive materials

associated with space applications of nuclear power systems are being investigated theoretically and experimentally. Interspecies comparative metabolic studies of radionuclides are continuing to provide needed data. Development, calibration, and use of external counting methods for the assessment of radioelement burdens in animals and man continue.

Radiation Genetics.--Studies of cumulative genetic effects in the progeny of successive generations of irradiated mice are now in the seventh year. After more than 35 generations of irradiation, differences in the progeny of the experimental and control lines are not particularly striking. Further analysis is required, but it is contemplated that termination of these studies will be started after the fortieth generation. Microbial and biochemical genetics efforts will be increased.

Molecular- and Cellular-Level Studies.--The molecular biology activity involves a very favorable consolidation of organic chemistry, biochemistry, and enzymology. Through combinations of chemical and enzymatic syntheses, model systems are available for detailed studies of biological information transfer reactions and the associated polymerase enzymes. The structure of histones and their possible function in this process are being investigated. Cellular biology activities are primarily concerned with establishing the temporal sequence of cellular processes in relation to specific portions of the life cycle. Extensive use is made of synchronized mammalian cells grown in suspension culture. Investigation of the mechanism of certain radiation effects will be started during the coming year. Studies of extracellular materials and cell surface phenomena will be somewhat increased. Electronic cell sizing, counting, and separating systems are being devised and improved in support of both the fundamental and programmatic biology programs, as well as automatic systems for continuous monitoring of the growth of tissue cultures.

(b) Terminations

The following terminations occurred during the present report period:

Miss R. L. DePriest, data analyst, Biophysics Section.

GROUP H-4

BIOMEDICAL RESEARCH

W. H. Langham, Ph.D., Leader
D. G. Ott, Ph.D., Alt. Group Leader
O. S. Johnson, B.S., Administrative Deputy
E. M. Sullivan, Group Secretary

MAMMALIAN METABOLISM

C. R. Richmond, Ph.D., Leader

Staff Member

J. E. Furchner, Ph.D.

Research Assistants

G. A. Drake, B.S.
J. S. Findlay, B.S.
J. E. London, B.S.

Technical Staff

S. Cordova
R. Martinez

*Casual employee.

MAMMALIAN RADIOBIOLOGY

J. F. Spalding, Ph.D., Leader

Staff Member

J. C. Hensley, D.V.M.

Research Assistants

M. R. Brooks, B.Ch.E.
C. F. Bidwell, M.S.

Technical Staff

R. C. Adams
F. Archuleta
R. F. Archuleta
J. E. Atencio
N. J. Basmann
A. M. Martinez, B.S.
L. Ortiz
A. Trujillo
F. Valdez
J. G. Valdez
E. A. Vigil

BIOPHYSICS

M. A. Van Dilla, Ph.D., Leader

Staff Members

P. N. Dean, M.A.
M. J. Fulwyler, B.S.
J. H. Larkins, B.S.*
J. D. Perrings

Research Assistant

J. M. Hardin, M.S.

Electronics Technician

L. J. Carr

CELLULAR RADIOBIOLOGY

D. F. Petersen, Ph.D.,
Leader

Staff Members

E. C. Anderson, Ph.D.
B. J. Barnhart, Ph.D.
I. U. Boone, M.D.**
R. R. J. Chaffee, Ph.D.
M. D. Enger, Ph.D.
C. T. Gregg, Ph.D.
E. A. Hyatt, Ph.D.
P. M. Kraemer, Ph.D.
A. G. Saponara, Ph.D.
R. A. Tobey, Ph.D.

Research Assistants

E. Campbell, B.S.
S. Carpenter, B.A.
S. H. Cox, B.A.
P. M. LaBauve, B.A.
P. C. Sanders, M.S.
F. Sapir, M.S.

Technical Staff

V. M. Gibbs, B.S.
J. L. Hanners

**Leave of absence.

MOLECULAR RADIOBIOLOGY

F. N. Hayes, Ph.D.
Leader

Staff Members

L. R. Gurley, Ph.D.
D. E. Hoard, Ph.D.
V. N. Kerr, M.A.
A. Murray, M.S.
R. L. Ratliff, Ph.D.
G. R. Shepherd, Ph.D.
D. A. Smith, Ph.D.
T. T. Trujillo, B.S.
D. L. Williams, M.S.

Research Assistants

G. T. Fritz, B.S.
E. Hansbury, M.A.
E. H. Lilly, B.S.
B. J. Noland, B.A.
C. N. Roberts, B.A.

Technical Staff

V. E. Mitchell

POSTDOCTORAL APPOINTEES

W. D. Currie, Ph.D.
A. W. Schwartz, Ph.D.

CHAPTER 4

BIOPHYSICS SECTION

ERYTHROCYTE VOLUME DISTRIBUTIONS DURING RECOVERY FROM BONE MARROW ARREST (M. A. Van Dilla, N. J. Basmann, J. M. Hardin, and J. F. Spalding)

INTRODUCTION

Some of the problems in electronic cell sizing and their solution have been discussed previously (1). We now apply the method to an experiment in the kinetics of erythropoiesis, in which bone marrow cell proliferation is suppressed for about 2 weeks by continuous irradiation. The changes in the volume distribution of the circulating red cells after release from the radiation exposure were studied and yielded information on the validity of the electronic sizing method and also on bone marrow response.

METHODS AND RESULTS

Twenty RF strain female mice were exposed to whole-body gamma irradiation at 5 rads/hr for 13.3 days for a total dose of 1600 rads. Previous experience has shown that this treatment causes bone marrow arrest, probably within the first few days of exposure. Blood samples were taken from 4 or 5 irradiated mice and 2 control mice at 2- to 4-day intervals during the 4-month recovery period to observe the replenishment of circulating erythrocytes. Red cell count and volume distribution were measured electronically. The experimental distributions were fit with an iterative least-squares code.

A skewed normal distribution (2) was found to fit the unimodal distributions better than a symmetrical normal curve. In cases such that the observed data were bimodal, the sum of two normal distributions was used because the extra two parameters required for the skewed functions made convergence difficult.

Figure 1 shows typical results; prior to the 13th day the volume distributions were similar to the controls but of smaller area (i.e., count) and mean (i.e., mean cell volume). The second population of large cells appeared between the 9th and 13th days after the end of exposure and increased in mean volume to a maximum on the 15th day. This population was identified as reticulocytes on microscopic examination of dry films made from these blood samples.

Figure 2 summarizes the results of the computer fits to all the experimental data. The parameters plotted are area, mean, and fractional standard deviation of the fitted functions all normalized to the control values so that they are dimensionless quantities, normally unity. Thus, they represent red cell count, mean cell volume (for each population when two are present), and variation in size of the red cells. The red cell count dropped to about half-normal at 10 days after the end of exposure and then slowly returned to near-normal. Mean cell volume was slightly (2 percent) below normal initially, falling steadily for about 10 days to 7 to 8 percent below normal, then rising rapidly to 30 percent above normal as the reticulocytes appeared; thereafter there was a slow decline to normal. The width of the distribution showed changes similar to the mean. The reticulocytes were 60 to 70 percent larger than normal red cells at first, and the mean volume of this abnormal population declined until it could no longer be resolved at about 30 days after the end of exposure. The mean cell volume of the normal population declined slightly, and then returned to normal (and overshot somewhat) as the reticulocytes appeared.

DISCUSSION

These results suggest the following conclusions:

(a) The volume distributions measured with a long aperture (30 μ in diameter and 225 μ long) seem to reflect accurately the actual red cell volume distributions existing in the blood. Normally, a single population is present and this is

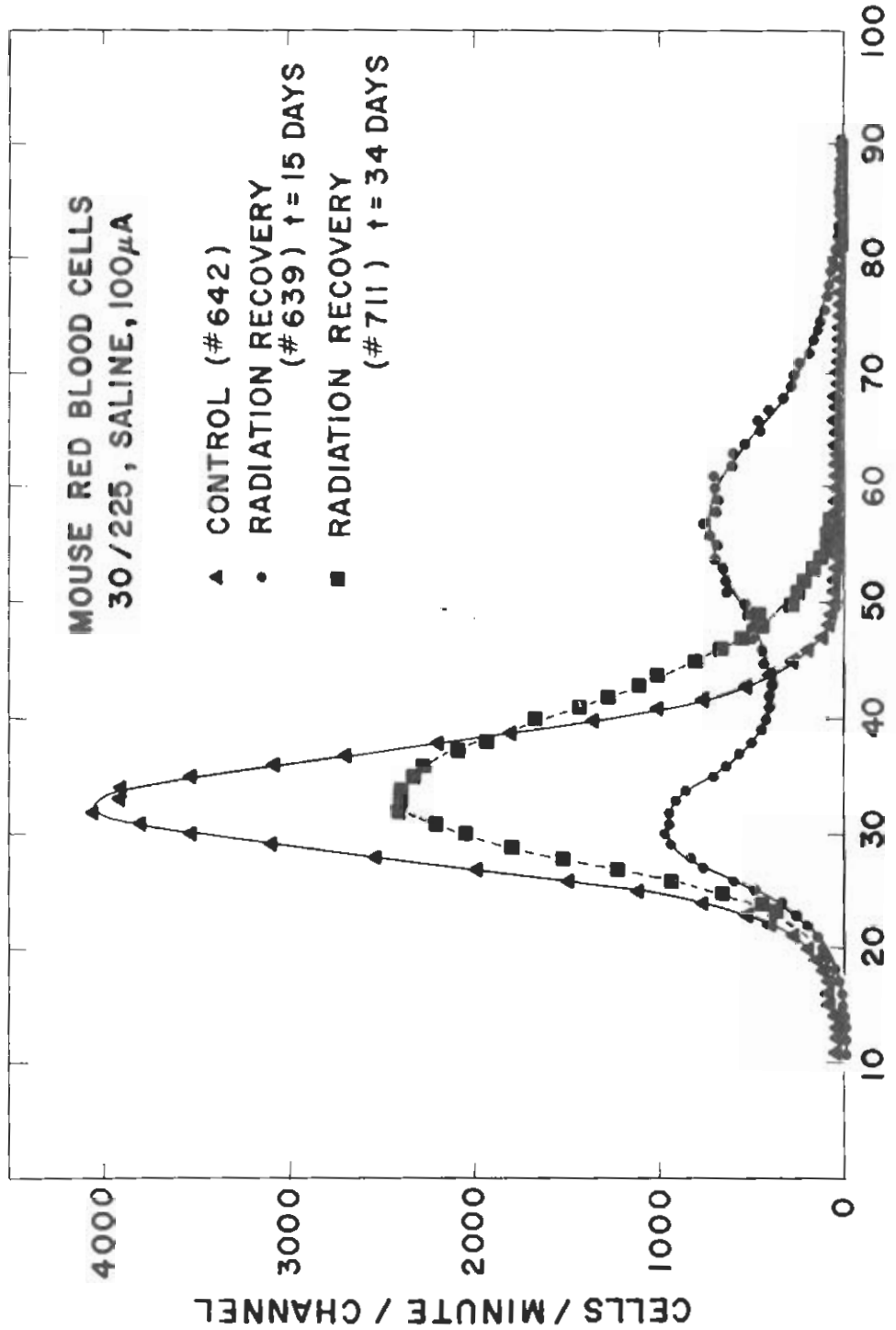

Fig. 1. Mouse red cell volume distribution 15 and 34 days post irradiation compared with control; dilution factor and volume of cell suspension measured are constant so that the areas under the curves are proportional to red cell count.

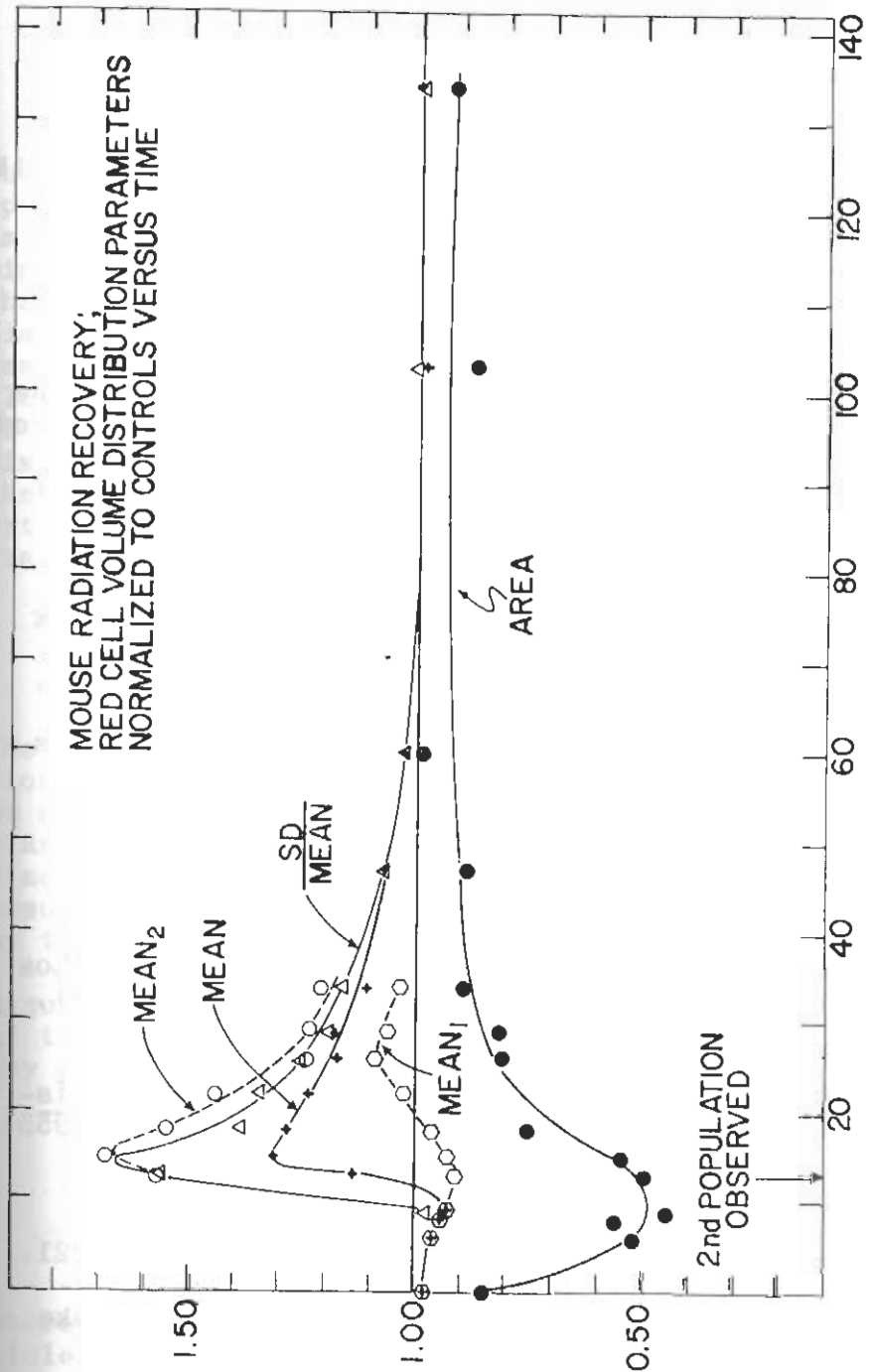

Fig. 2. Variation of computer-derived red cell volume distribution parameters with time after end of gamma-ray exposure, normalized to control values. Curve labels have the following meaning: area is red cell count; mean$_1$ is mean cell volume of normal population; mean$_2$ is mean cell volume of macrocytic reticulocytes; mean is mean cell volume of total population; and SD is standard deviation.

also the result given by the electronic sizing procedure. When a second population of larger cells is present (as proved by microscopic examination), this population is clearly observed in the measured volume distributions. In addition, the number of reticulocytes obtained from slide counts agrees with that from electronic sizing.

(b) The volume distribution of normal mouse red cells is well described by a skewed normal function with only a slight asymmetry to the large volume side. The skewness parameter (α_3 in Ref. 2) is in the range of 0.1 to 0.3.

(c) The macrocytic reticulocytes seem to be the same as previously reported by Brecher and Stohlman (3) and Seno et al. (4) as a result of other stimuli such as phenylhydrazine and bleeding. Apparently the severe need for circulating red cells results in the skipping of a terminal cell division, leading to macrocytosis followed by replacement by cells of more normal size.

(d) If it is assumed that red cell production was reduced by the radiation exposure, then mean age of the circulating erythrocytes gradually increased until appearance of the reticulocytes. Since mean volume decreased simultaneously, it follows that red cell volume decreases with age (it has been previously established that red cell density increases with age).

REFERENCES

(1) M. A. Van Dilla, N. J. Basmann, and M. J. Fulwyler, Los Alamos Scientific Laboratory Report LA-3132-MS (1964), p. 182.

(2) F. E. Croxton and D. J. Cowden, Applied General Statistics, Prentice Hall, Englewood Cliffs, New Jersey (1955), p. 619.

(3) L. O. Jacobson and M. Doyle, eds., Erythropoiesis, Grune and Stratton, Inc., New York (1962), pp. 216-221.

(4) S. Seno, M. Miyahara, H. Asakuru, O. Ochi, K. Matsuska, and T. Toyama, Blood 24, 582 (1964).

FLOW OF PARTICLES THROUGH A COULTER APERTURE: HYDRODYNAMIC CONSIDERATIONS (F. H. Harlow* and M. A. Van Dilla)

INTRODUCTION

When very uniform polystyrene spheres flow through a Coulter aperture of such dimensions that their transit time approximates the rise time of the pulse amplifier, a distorted bimodal pulse-height distribution results (1). The detailed shape of this distribution is a function of particle transit time. It appears that this type of distribution can be at least partly accounted for by the pattern of hydrodynamic flow through the aperture and the rise time characteristic of the amplifier. Theoretical analysis of the transit time distribution imposed by the boundary layer and fluid core in the region of unestablished flow in a short pipe (i.e., aperture) leads to a bimodal distribution which approximates what is observed experimentally.

METHODS AND RESULTS

The theoretical treatment which follows contains simplifications to make the mathematics tractable; only an outline will be given in the interests of conserving space. The general plan is: (a) calculation of the distribution of transit times; and (b) calculation of the pulse-height distribution resulting from modification of the transit time distribution by the response of the amplifier.

Assuming that fluid flow through the aperture is laminar and if t equals transit time and u(r,z) equals fluid velocity at any point in the aperture, then

$$t = \int_0^L \frac{dz}{u(r,z)} , \qquad \text{(Eq. 1)}$$

where the geometry is shown in Fig. 1. If the incoming particle distribution is uniform and N particles enter during an

---

*LASL Theoretical Division.

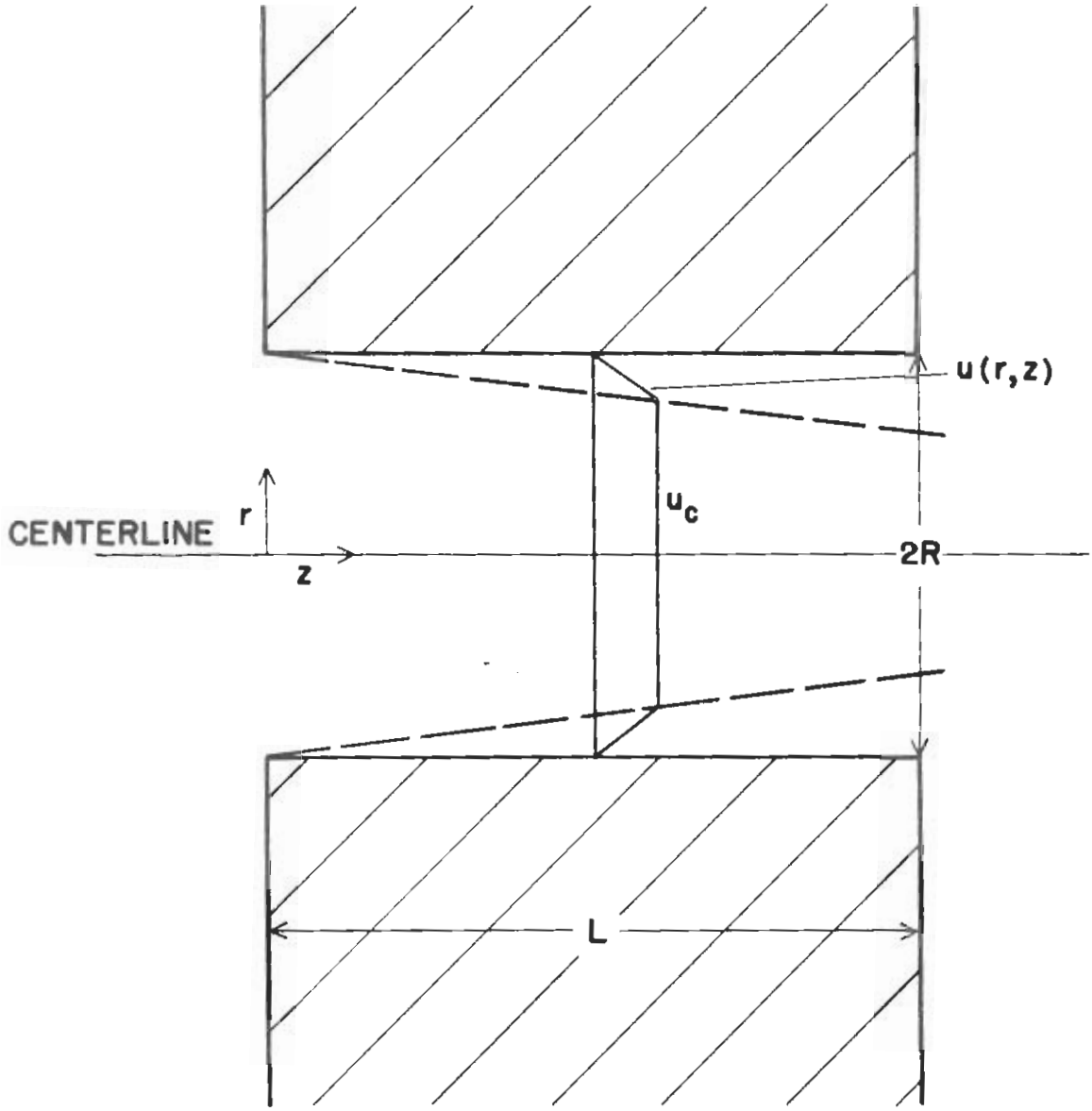

Fig. 1. Aperture cross section showing coordinate system and velocity profile.

experiment, then the number of particles traversing between r and r + dr is

$$N(r)\ dr = N\ \frac{2\pi\ r\ dr}{\pi\ R^2} = \frac{2\ Nr}{R^2}\ dr.$$

The difference in transit time across the radius interval dr is

$$dt = -\int_0^L \left[\frac{dz}{u^2\ (r,z)}\ \frac{\delta u(r,z)}{\delta r}\right]\ dr.$$

But

$$\left[N(t)\ dt = N(r)\ dr\right] = \frac{2\ Nr}{R^2\int_0^L\left[\frac{1}{u^2\ (r,z)}\ \frac{\delta u(r,z)}{\delta r}\ dz\right]}\ dt, \qquad \text{(Eq. 2)}$$

where N(t) is the transit time distribution function desired. Assume the pulse amplifier response to a step function input is

$$P(t) = P_o\ (1 - e^{-t/\tau}), \qquad \text{(Eq. 3)}$$

where τ is the amplifier rise time. Then

$$N(P)\ dP = N(t)\ dt, \qquad \text{(Eq. 4)}$$

where N(P) is the desired pulse-height distribution function in parametric form. The next part of the problem, then, is to find workable expression for the velocity, u(r,z).

The case of importance is the aperture of length equal to diameter of 30 μ, which has been shown to give a highly distorted bimodal distribution for uniform spheres. For this aperture the boundary layer (2) does not extend to the center line (i.e., the flow is unestablished), and we make the approximation that the velocity is proportional to distance from the wall out to the transition interface (3) and constant to the center line:

$$u(r,z) = u_c = \text{constant (central region)}$$

$$u(r,z) = (R - r)\left(u_c \sqrt{\frac{u_c}{\pi \nu z}}\right) \text{ (boundary layer)},$$

where u_c = center line velocity and ν = viscosity. Substituting in Eq. (1), neglecting the term in $(R - r)^2$, and then using Eq. (2) results in the following transit time distribution:

$$\frac{\alpha N L}{u_c} \frac{1}{t^2}, \text{ for } t > t_{min} = \frac{L}{u_c}$$

$$N(t) = \text{constant} \times \delta (t - t_{min}), \text{ for } t = t_{min}$$

$$0, \text{ for } t < t_{min}$$

where constant $= N(1 - \alpha)$, $\alpha = \frac{4\sqrt{\pi}}{3} \sqrt{\frac{L}{R} \frac{1}{R_e}}$, R_e = Reynolds' number $= \frac{u_c R}{\nu}$, and δ = delta function.

The final step is the modification of this transit time distribution by the response of the amplifier. To do this we combine the expressions for N(t) with Eqs. (3) and (4). For $t > t_{min}$, the result is

$$\frac{P_o}{N} N(P) = \frac{\alpha L}{u_c \tau} \frac{1}{(1 - \lambda) \ln^2 (1 - \lambda)}$$

$$\lambda = P/P_o,$$

and for $t = t_{min}$, the result is

$$\frac{P_o}{N} N(P) = \frac{1 - \alpha}{0.2} = 3.63,$$

where a delta function width of 0.2 has been assumed and $L = 2R = 3 \times 10^{-3}$ cm, $u_c = 10^3$ cm/sec, and $v = 10^{-2}$ stoke (which are typical aperture conditions). A plot of this result (Fig. 2) shows the general features of the resultant pulse-height distribution: (a) bimodal shape; (b) peak at minimum pulse-height due to particles traversing aperture in minimum time (central region of flow); and (c) peak at maximum pulse-height due to particles traversing aperture more slowly (boundary layer).

In practice, both peaks will be broadened and blurred into smooth curves by such effects as amplifier noise, turbulence, and possible radial component of particle velocity. But it does seem that this rough approach shows how uniform particles can produce a spurious, bimodal pulse-height distribution with varying areas in each peak as hydrodynamic parameters change.

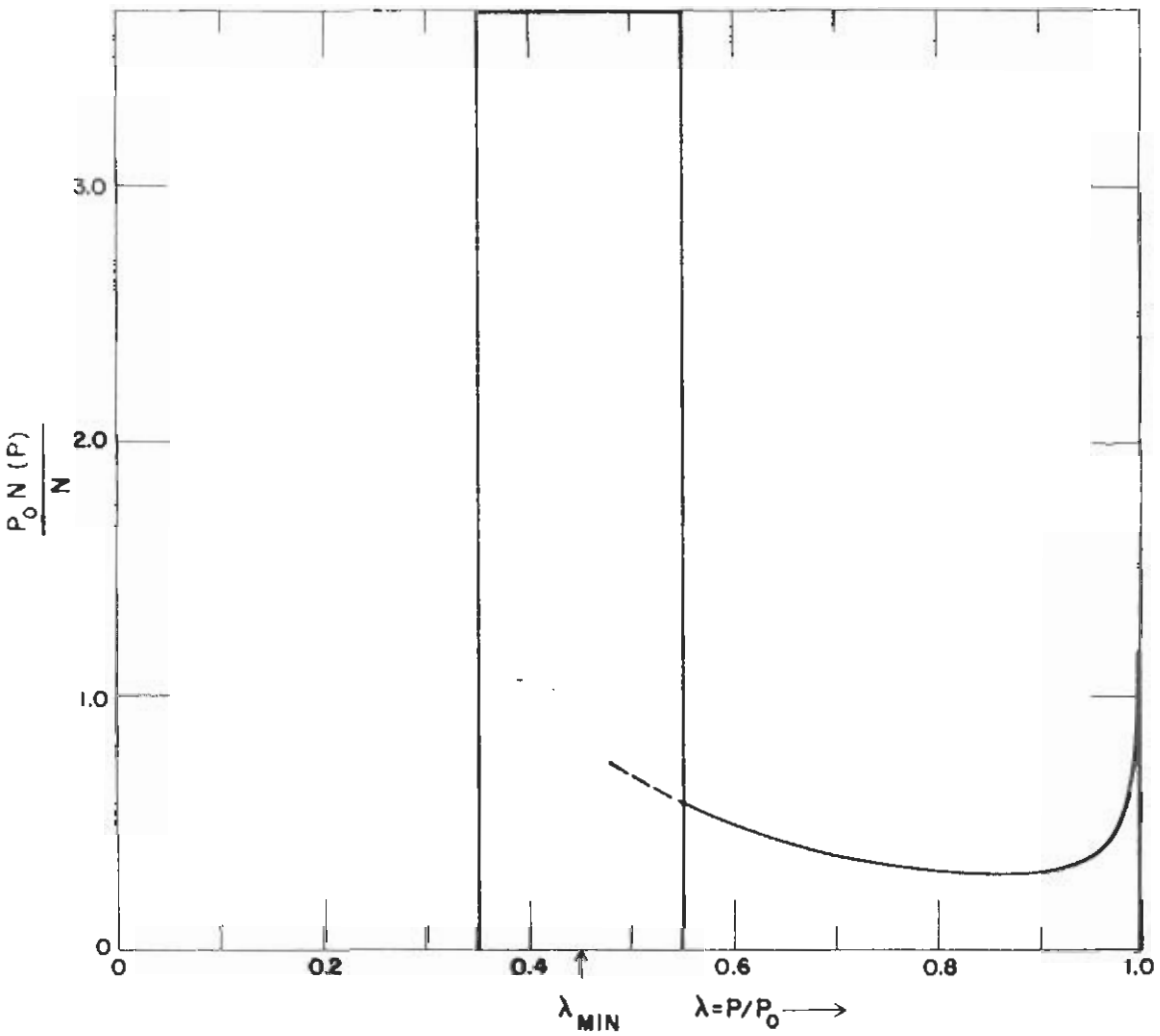

Fig. 2. Theoretical pulse-height distribution for an aperture of length equal to diameter of 30 μ traversed by uniform particles.

REFERENCES

(1) M. A. Van Dilla, N. J. Basmann, and M. J. Fulwyler, Los Alamos Scientific Laboratory Report LA-3132-MS (1964), p. 190.

(2) J. K. Vennard, Elementary Fluid Mechanics, Wiley and Sons, New York (1961), pp. 244-247.

(3) V. L. Streeter, ed., Handbook of Fluid Dynamics, McGraw-Hill, New York (1961), Section 9, p. 11.

AN ELECTRONIC PARTICLE SEPARATOR WITH POTENTIAL BIOLOGICAL APPLICATION (M. J. Fulwyler)

INTRODUCTION

The particle separator is a device which, in principle, is capable of separating microscopic particles according to an electronically measurable characteristic such as volume, optical density, or fluorescence. Separation is accomplished as follows. The particle, in liquid suspension, passes by a sensor which measures the characteristic of interest. The suspension is forced through a nozzle and emerges as a jet which is broken into droplets, thereby isolating the suspended particles. The droplets containing the particles of interest are charged and then deflected by an electrostatic field into a collection vessel.

METHOD

Shown in Fig. 1 is a device which is being developed to separate particles according to their volume. A cell suspension (under 4 atmospheres pressure) enters the droplet generator (C) via a tube (D) and emerges as a high-velocity fluid jet (E) [diameter 36 μ, velocity 15 m/sec]. A piezoelectric crystal (A), driven at a frequency of 72,000 c/sec, produces vibrations which pass down the Lucite rod (B) into the liquid within the droplet generator. The catenoidal shape of the rod amplifies the magnitude of the vibrations within the liquid, and the velocity fluctuations of the emerging liquid cause the jet to break into 72,000 very uniform droplets each second.

Droplets are charged as they pull away from the charged liquid column by applying a voltage at (K) relative to (M), which is in contact with the emerging stream. As the droplet separates, it carries away a charge proportional to the instantaneous charge on the column of liquid. In this way one or more droplets may be charged. The charged droplets are deflected (H) on entering the electrostatic field (7,000 volts/cm) between the deflection plates (G). A series of collection vessels (L) receives the deflected droplets.

The sequence of events leading to separation is as follows. Cell volume is sensed as the cell passes through a Coulter

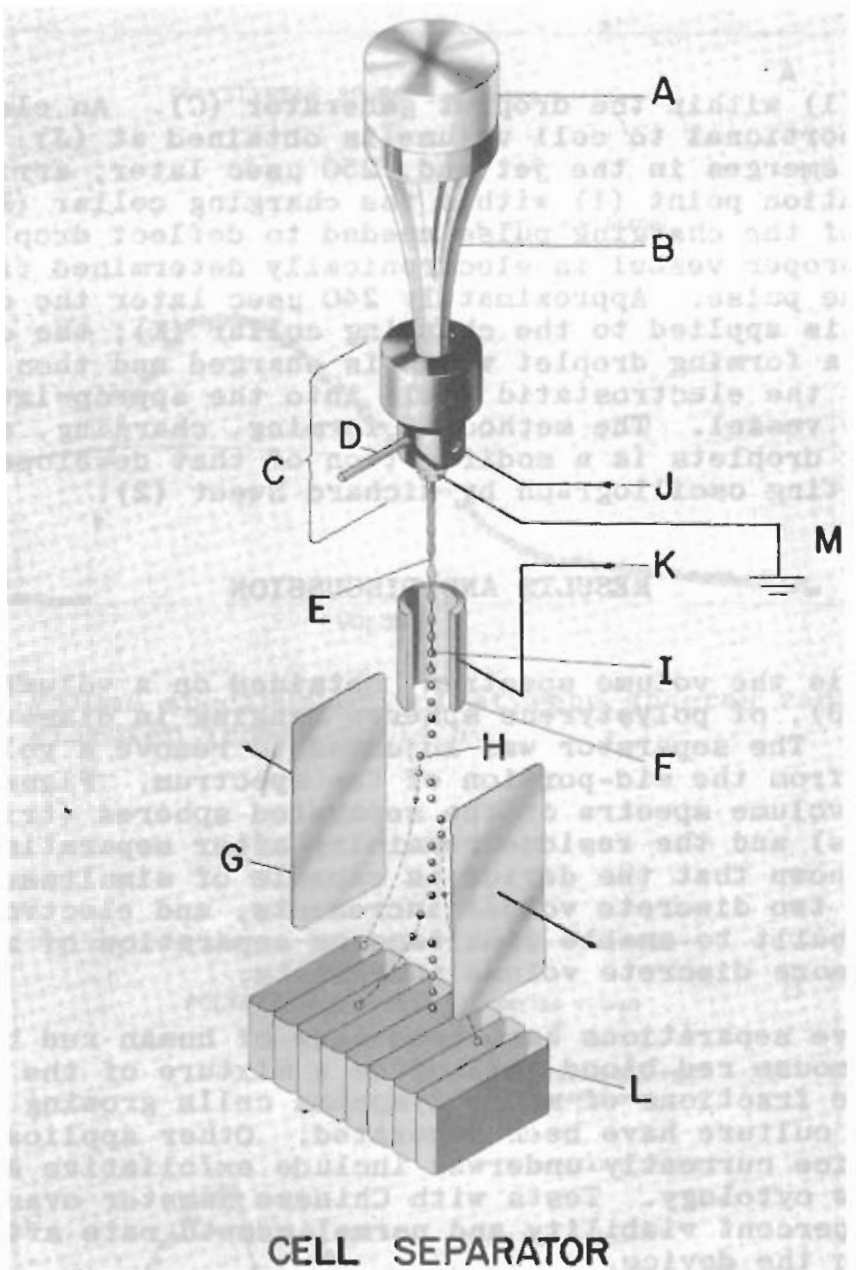

Fig. 1. Cell separator: (A) piezoelectric crystal; (B) acoustic coupling rod; (C) droplet generator; (D) fluid entry tube; (E) fluid jet; (F) charging collar; (G) electrostatic deflection plates; (H) deflected droplets; (I) droplet separation point; (J) cell volume signal contact; (K) charging collar contact; (L) droplet collection system; and (M) ground contact for emerging jet.

aperture (1) within the droplet generator (C). An electric pulse proportional to cell volume is obtained at (J). The cell then emerges in the jet and, 250 μsec later, arrives at the separation point (I) within the charging collar (F). The size of the charging pulse needed to deflect droplets into the proper vessel is electronically determined from the cell volume pulse. Approximately 240 μsec later the charging pulse is applied to the charging collar (K); the cell is caught in a forming droplet which is charged and then deflected by the electrostatic field into the appropriate collection vessel. The method of forming, charging, and deflecting droplets is a modification of that developed as an ink-writing oscillograph by Richard Sweet (2).

RESULTS AND DISCUSSION

Figure 2A is the volume spectrum, obtained on a volume spectrometer (3), of polystyrene spheres ranging in diameter from 7 to 14 μ. The separator was adjusted to remove a volume increment from the mid-portion of the spectrum. Figure 2B shows the volume spectra of the separated spheres (triangular data points) and the residue remaining after separation. It has been shown that the device is capable of simultaneously separating two discrete volume increments, and electronics are being built to enable simultaneous separation of a sample into 6 or more discrete volume increments.

Quantitative separations have been made of human red blood cells and mouse red blood cells from a mixture of the two. Also volume fractions of mouse lymphoma cells growing in suspension culture have been separated. Other applications of the device currently underway include exfoliative and bone marrow cytology. Tests with Chinese hamster ovary cells showed 96 percent viability and normal growth rate after passing through the device.

Development and refinement of the device are proceeding. Separations under sterile conditions are expected in the near future. Investigation is underway of a sensor system able to measure optical characteristics of a particle. With such a system, it may be possible to measure simultaneously two (or more) characteristics of a cell and to make separation dependent on the relation of these two characteristics.

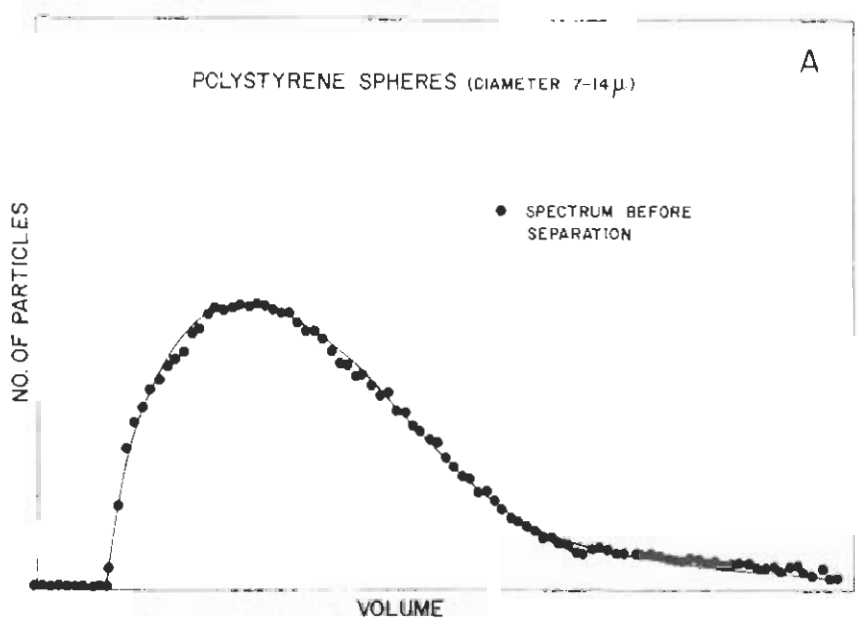

Fig. 2A. Volume spectrum of polystyrene spheres ranging in diameter from 7 to 14 μ.

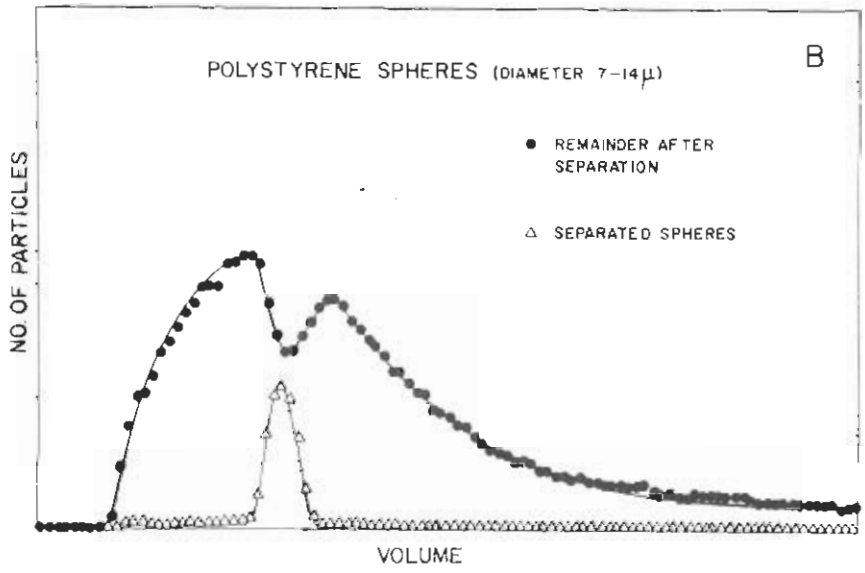

Fig. 2B. Volume spectrum of separated spheres (triangles) and the volume spectrum of the residue after separation (solid points).

REFERENCES

(1) W. H. Coulter, U. S. Patent No. 2,656,508 (1953); W. H. Coulter, Proceedings of the National Electronics Conference 12 (1956), p. 1034.

(2) R. G. Sweet, Stanford University Technical Report 1722-1. Available from Defense Document Center, Washington, D. C., Report SU-SEL-64-004 (1964).

(3) M. A. Van Dilla, N. J. Basmann, and M. J. Fulwyler, Los Alamos Scientific Laboratory Report LA-3132-MS (1964), p. 182.

EXPERIMENTAL TECHNIQUE FOR HIGH PRECISION CALIBRATION OF WHOLE-BODY COUNTERS: APPLICATION TO A 4π LIQUID SCINTILLATOR AND A LARGE SODIUM IODIDE (Tl) CRYSTAL SPECTROMETER, P. N. Dean. In: Radioactivity in Man (G. R. Meneely and S. M. Linde, eds.), Charles C. Thomas, Publ., Springfield, Ill. (1965), pp. 94-103.

With the 4π liquid scintillator, potassium determinations can be made on random subjects to a precision of ± 2.1 percent based on the calibration alone. Including statistics, the precision is ± 3.0 percent for a counting time of 200 sec.

With the crystal spectrometer, potassium determinations can be made on random subjects to a precision of ± 2.7 percent based on the calibration alone. Including statistics, the precision is ± 3.5 percent for a counting time of 50 min.

ERYTHROCYTE SIZE DISTRIBUTIONS FOLLOWING RADIATION-INDUCED BONE MARROW ARREST, M. A. Van Dilla, J. M. Hardin, N. J. Basmann, and J. F. Spalding. Radiation Res. 25, 79 (1965), Abstract No. 209.

The principle of cell counting invented by W. H. Coulter has been extended to red cell sizing. The size distribution of erythrocytes in normal people and mice is shown to be unimodal, approximately normal with a standard deviation of close to 15 percent. Using improper aperture conditions, however, spurious bimodal distributions are obtained which can lead to the notion that two volumetrically distinct populations are present in the blood of normal individuals. The reasons for these artifacts are not clear, but they are avoided by proper choice of aperture dimensions, cell transit time, and by using minimum aperture current. In an experiment on bone marrow arrest, mice were exposed to a gamma-ray dose of 5 rads/hr for 14 days, after which they were removed to allow resumption of bone marrow activity. Red cell sizing began at the end of exposure; in the following 2 weeks red cell concentration dropped to 50 percent of normal while mean cell volume and fractional standard deviation dropped from 2 to 7 percent below normal. Then a sudden release of immature red cells into the circulation was observed. A second oversized population of 60 to 70 percent greater volume appeared, reversing the downward trend of red cell concentration and causing the mean cell volume to rise

to 30 percent over normal and the fractional standard deviation to increase to 65 percent over normal. In the following weeks the second population diminished in concentration and size; mean cell volume and fractional standard deviation returned to normal while red cell concentration climbed to within 5 to 10 percent of normal.

RADIOACTIVE CONTAMINATION OF CONTEMPORARY LEAD, R. I. Weller, E. C. Anderson, and J. L. Barker. Nature 206(4990), 1211-1212 (1965).

A study of the gamma-ray activity of 8 samples of commercial lead showed that 3 of them were equivalent to the best "aged" lead for low-level shielding. The contaminant in the other 5 was identified as lead-210 plus daughters at concentrations up to 38 nc/kg. The results indicate that selected commercial lead can be used where ultimate shielding quality is required.

RADIATION BIOLOGY AND SPACE ENVIRONMENTAL PARAMETERS IN MANNED SPACECRAFT DESIGN AND OPERATIONS, W. H. Langham, P. M. Brooks, and D. Grahn, eds. Aerospace Med. 36(2), Section II (1965), 55 p.

The purpose of this report is to derive, insofar as possible, criteria for consideration of man's response to space radiation exposure so that radiation risks may be taken into account, during spacecraft design and operational planning phases, along with the other inherent hazards of manned space flight. The only basis for derivation of such criteria is the vast amount of data on effects of so-called conventional radiation exposures (involving low and intermediate energy electromagnetic and particulate radiations) on animals and occasionally man. Unfortunately, exposures in space will not be conventional either with regard to exposure conditions or nature, energy, and spectral distribution of the radiations. It seems necessary, therefore, to discuss first some of the general and specific aspects of the space radiation environment and some of the exposure conditions that may be contemplated.

attention to metabolic studies. All of the above -- data acquisition, reduction and analysis -- have proven to be indispensable to programmatic research of the Biomedical Research Group of the Los Alamos Scientific Laboratory.

SOME BIOLOGICAL ASPECTS OF RADIOACTIVE MICROSPHERES, W. H. Langham, C. R. Richmond, J. C. Hensley, P. N. Dean, and M. A. Van Dilla. Los Alamos Scientific Laboratory Report LA-3365-MS (in press).

The effectiveness of particle size control as a means of alleviating the potential radioactive particle inhalation hazards inherent in space use of nuclear power systems will depend on a variety of factors, among which are biological effects produced by radioactive particles too large to enter the respiratory tract. If insoluble, such particles will constitute discrete radiation sources. Discrete sources deposited on the skin surface may produce significant lesions and, if swallowed, may result in irradiation of the gastrointestinal mucosa during passage. If soluble, the radioactive materials present may be absorbed into the body or enter the ecological cycle, resulting in an internal source of radiation exposure. This report covers some preliminary observations believed pertinent to assessing the biological effects of discrete radiation sources, particularly fissioned uranium-235 carbide microspheres in the size range of about 100 to a few hundred microns.

COMPUTER REDUCTION OF METABOLIC DATA OBTAINED FROM SCINTILLATION COUNTERS, P. N. Dean. Los Alamos Scientific Laboratory Report LA-3298 (in press).

This report describes in detail the RTW series of computer programs written to analyze metabolic data. The programs calculate elapsed time between radionuclide administration and time of measurement, correct all data for changes in counting efficiency relative to measurements made on standards at zero time and for physical decay, if desired, and express the observed counting information as effective or biological retention at time of measurement.

ELECTRONIC SEPARATION OF BIOLOGICAL CELLS BY VOLUME, M. J. Fulwyler. Science (in press).

A device has been developed which is capable of separating biological cells (suspended in a conducting medium) according to volume. Cell volume is measured in a Coulter aperture, and the cells are subsequently isolated in droplets of the medium which are charged according to the sensed volume. The charged droplets then enter an electrostatic field and are deflected into a collection vessel. Mixtures of mouse and human erythrocytes and a large volume component of mouse lymphoma cells were separated successfully. In tests with Chinese hamster ovary cells, essentially all survived separation and grew at their normal rate.